

ARTICLE TYPE

Cite this: DOI: 00.0000/xxxxxxxxxx

Dual mechanism of ionic liquid-induced protein unfolding[†]

Onkar Singh, a^{\ddagger} Pei-Yin Lee, b^{\ddagger} Silvina Matysiak, *c and Harry Bermudez *a

Received Date Accepted Date

DOI: 00.0000/xxxxxxxxxx

Ionic liquids (ILs) are gaining attention as protein stabilizers and refolding additives. However, varying degrees of success with this approach motivates the need to better understand fundamental IL-protein interactions. A combination of experiment and simulation is used to investigate the thermal unfolding of lysozyme in the presence of two imidazolium-based ILs (1-ethyl-3-methylimidazolium ethylsulfate, [EMIM][EtSO₄] and 1-ethyl-3-methylimidazolium diethylphosphate, [EMIM][Et₂PO₄]). Both ILs reduce lysozyme melting temperature T_m , but more gradually than strong denaturants. $[EMIM][Et_2PO_4]$ lowers lysozyme T_m more readily than $[EMIM][EtSO_4]$, as well as requiring less energy to unfold the protein, as determined by the calorimetric enthalpy ΔH . Intrinsic fluorescence measurements indicate that both ILs bind to tryptophan residues in a dynamic mode, and furthermore, molecular dynamics simulations show a high density of [EMIM]⁺ near lysozyme's Trp62 residue. For both ILs approximately half of the [EMIM]+ cations near Trp62 show perfect alignment of their respective rings. The [EMIM]+ cations, having a "local" effect in binding to tryptophan, likely perturb a critically important Arg-Trp-Arg bridge through favorable $\pi-\pi$ and cation- π interactions. Simulations show that the anions, $[EtSO_4]^-$ and $[Et_2PO_4]^-$, interact in a "global" manner with lysozyme, due to this protein's strong net positive charge. The anions also determine the local distribution of ions surrounding the protein. [Et₂PO₄] is found to have a closer first coordination shell around the protein and stronger Coulomb interactions with lysozyme than $[EtSO_4]^-$, which could explain why the former anion is more destabilizing. Patching of ILs to the protein surface is also observed, suggesting there is no universal IL solvent for proteins, and highlighting the complexity of the IL-protein environment.

Introduction

Due to the importance of proteins in food, catalysis ¹, and biomedicine ², many efforts in recent years have explored ionic liquids (ILs) to modulate protein behavior ^{3,4}. There is also interest in the long-term preservation of proteins without refrigeration ⁵. To this end, substantial efforts have been undertaken to explore protein behavior in IL-water mixtures, usually with a focus on model globular proteins such as lysozyme ^{6,7}, ribonuclease A^{8,9}, cytochrome c ^{10,11}, hemoglobin ¹², and lipases ^{13,14}. In spite of these efforts no general trend has emerged for how ILs modulate protein stability, suggesting the need for a closer examination of specific protein-IL pairings.

It is important to note that in many reports the amount of

Several recent works examined lysozyme behavior specifically with significant IL content. Most notable is the early work by Byrne et al. ²⁰ who demonstrated multi-year structural stabilization, as confirmed by calorimetry, by using a mixture of 27 wt% sucrose and 31 wt% ethylammonium nitrate. Mann et al. ¹⁸ studied the ability of several related ammonium formate ILs to promote lysozyme refolding after thermal denaturation. Ethanolammonium formate performed particularly well at this task, and when at concentrations greater than 50 wt% it also improved lysozyme thermal stability. Weaver et al. ²¹ studied the effect of choline dihydrogenphosphate and found an increase in lysozyme thermal stability with increasing concentration (up to 40 wt%). The above papers suggest an important role for the hydroxyl group of the cation (ethanolammonium and choline), and yet anions are well known to contribute to protein behavior ^{3,8,22}. In-

IL $^{15-17}$ and/or the protein concentration 8,10,18 can be quite low, such that the solutions are largely dilute and aqueous. One benefit of such conditions is that changes in protein stability can be interpreted within the context of Hofmeister series 19 and/or electrostatic screening effects. However, when the goal is to enhance ambient and long-term protein stability, it is questionable if dilute conditions are relevant.

^a Department of Polymer Science and Engineering, University of Massachusetts, Amherst, MA, USA. Tel: +1 413 577 1413; E-mail: bermudez@umass.edu

^b Chemical Physics Program, Institute for Physical Science and Technology, University of Maryland, College Park, USA.

^c Fischell Department of Bioengineering, University of Maryland, College Park, USA. Tel: +1 301 405 0313; E-mail: matysiak@umd.edu

 $[\]dagger$ Electronic Supplementary Information (ESI) available. See DOI: 10.1039/cXCP00000x/

[‡] These authors contributed equally to this work.

deed, Rodrigues et al. ²³ used ILs of choline paired with various anions to show that lysozyme thermal stability could be strongly affected (either increase or decrease) depending on the anion. It becomes clear that there is a need for closer examination of *both* IL ions on protein behavior, and a focus on either cation or anion alone is likely to be insufficient.

Another limitation to our understanding is that molecular insights are often still lacking, especially in the cases where proteins are destabilized. For example, the details of the unfolding process also remain largely unexplored: do proteins partially unfold? Is the unfolding process cooperative, reversible? Considering specific pairings of proteins and ILs, what molecular interactions are responsible for the observed behavior? These types of questions can be answered more thoroughly through a combination of experiment and simulation, taking advantage of the benefits from each approach. Molecular dynamics (MD) simulation is uniquely suited to provide a wealth of detailed information, such as atomic-scale structure and microscopic kinetics. MD also allows us to study the IL organization near the protein surface, as well as short and long-range interactions between the ions and the protein.

Towards the goal of understanding the effect of ILs on protein stability, here we use a combination of experiment and simulation to investigate the behavior of a model protein, lysozyme, in the presence of two different ILs, 1-ethyl-3-methylimidazolium ethylsulfate and 1-ethyl-3-methylimidazolium diethylphosphate. These ILs are chosen due to their miscibility with water and because sulfate and phosphate anions have relevance to protein-protein interactions ²⁴.

Experimental

Materials and Methods

1-ethyl-3-methylimidazolium ethylsulfate [EMIM][EtSO $_4$] (\geq 95%), 1-ethyl-3-methylimidazolium diethylphosphate [EMIM][Et $_2$ PO $_4$] (\geq 98%), and lysozyme (\geq 90%) from chicken egg white were purchased from Sigma-Aldrich. All chemicals were used as received.

Sample Preparation

Lysozyme solutions (10 wt%) were prepared by dissolving 30 mg of lysozyme in 270 mg of various IL-water (17 to 75 wt%) mixtures.

Calorimetry

Differential scanning calorimetry (DSC) measurements were performed with a TA Q100 with refrigerated cooling system. Approximately 10 mg of solution was hermetically sealed in an aluminum pan and an empty pan used as a reference. For measuring the unfolding temperature T_m , samples were heated from 293 to 373 K with a heating rate of 2 K/min. The instrument was calibrated using sapphire and indium. Every experiment was repeated thrice, and average value reported.

Fluorescence Spectroscopy

A photoluminescence spectrometer from Photon Technology International was used for the fluorescence measurements. The intrinsic fluorescence of lysozyme was monitored with an excitation wavelength of 280 nm in quartz cuvette having a path length of 10 mm. The emission spectra were recorded between 285 to 485 nm keeping the excitation and emission slit widths at 0.5 mm. All above experiments were performed at room temperature.

Simulations

Three systems containing lysozyme (water, wt% [EMIM][EtSO₄] and 25 wt% [EMIM][Et₂PO₄]) were simulated with all-atom molecular dynamics using Gromacs 2018 package ²⁵. For the starting protein structure, the coordinates of chicken egg white lysozyme of Protein Data Bank (PDB) entry 1AKI was taken with all crystallographical water molecules removed. OPLS-AA force field 26 was used for lysozyme, water and chloride ions. A non-polarized force field developed by Canongia et al²⁷, which was compatible with the OPLS-AA force field was used for [EMIM]+ and [EtSO₄]- ions. LigParGen server was used to generate force field parameters that were also compatible with OPLS-AA forced field for $[Et_2PO_4]^{-28}$. The details of validation of these parameters are described in the supplemental information. The pH of the systems were set at 7 to match experimental conditions of water. For the water system, lysozyme was solvated in a $7.01 \times 7.01 \times 7.01 \text{ nm}^3$ cubic box with 10636 SPC water molecules and 8 chloride ions to neutralize the system. For the 25 wt% [EMIM][EtSO₄] system, lysozyme was solvated in a $8.50 \times 8.50 \times 8.50 \text{ nm}^3$ cubic box with 9041 SPC water molecules, 8 chloride ions, 230 [EMIM]+ ions and 230 [EtSO₄] ions. For the 25 wt% [EMIM][Et₂PO₄] system, lysozyme was solvated in a $8.00 \times 8.00 \times 8.00 \text{ nm}^3$ with 8456 SPC water molecules, 8 chloride ions, 192 [EMIM]+ ions, and 192 $[Et_2PO_4]^-$ ions. The molecular structures for all IL ions are shown in Figure 1.

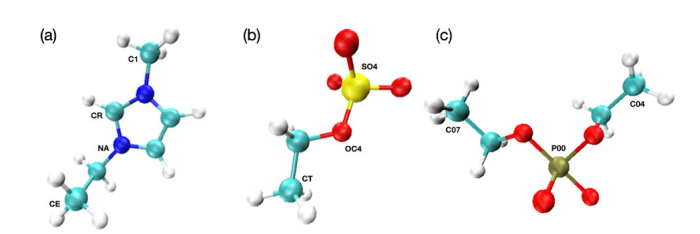


Fig. 1 Molecular structures of (a) [EMIM] $^+$ cation, (b) [EtSO $_4$] $^-$ anion, and (c) [Et $_2$ PO $_4$] $^-$ anion. White: hydrogen; cyan: carbon; blue: nitrogen; red: oxygen; yellow: sulfur; and tan: phosphorus. The marked atoms are for the identification purpose in Figure 7.

Prior to production runs, the energy of the system was minimized using the steepest descent method, followed by isochoric-isothermal (NVT) and isobaric-isothermal (NPT) ensemble runs of 100 ps each and at 300 K. Pressure for NPT equilibration was set at 1 bar. The volumes of the simulation boxes after initial equilibration were $6.96 \times 6.96 \times 6.96$ nm³, $7.12 \times 7.12 \times 7.12 \times 7.12$ nm³, and $6.98 \times 6.98 \times 6.98$ nm³ for water, 25 wt% [EMIM][EtSO₄], and 25 wt% [EMIM][Et₂PO₄] system, respectively. As for the

production run, a total of 9 trajectories have been run for 1 µs for the three systems and at 3 temperatures (300 K, 370 K, and 400 K). All production runs were run with NPT ensemble with a time step of 2 fs and pressure at 1 bar. Linear Constraint Solver Algorithm (LINCS) was used for the constraint algorithm and all bonds involving hydrogens were constrained. The cutoff for both short range Coulomb and van der Waals interactions was 1.0 nm. These cutoff values were also used to calculate the short range interactions between lysozyme and ILs. Typically a cutoff between 0.8 to 1.2 nm is used. Although longer cutoff values are desirable, 1.0 nm is chosen because of the desire of better sampling.²⁹ The particle-mesh Ewald method 30 was used for the long-range electrostatic interactions. Parrinello-Rahman barostat31 and Vrescale thermostat were used to control pressure and temperature, respectively. The compressibilities of the system were set to $4.50 \times 10^5 \text{ bar}^{-1}$, $4.23 \times 10^5 \text{ bar}^{-1}$, and $4.23 \times 10^5 \text{ bar}^{-1}$ for water, 25 wt% [EMIM][EtSO₄], and 25 wt% [EMIM][Et₂PO₄] systems, respectively, to reflect different solvent compressibility between water and IL/water mixtures 32.

The last 800 ns data were used for analysis. Native contact pairs were first determined by selecting two atoms that are more than four residues away but less than 0.75 nm in distance from 1AKI.pdb structure. The pair list was then used to determine the fraction of native contacts of a structure with the same cutoff of 0.75 nm. Potential mean force (PMF) was calculated based on eq.1, where W(rxn) is the PMF of a reaction coordinate (rxn) and P is the probability distribution of that rxn.

$$W(rxn) = -\ln P(rxn) \tag{1}$$

The probability distribution of the absolute cosine angle between the normal of [EMIM] $^+$ rings near Trp62 and the normal of Trp62 ring is also calculated. An [EMIM] $^+$ is considered to be near Trp62 if its CR atom (Figure 1) is within a cutoff of 0.4 nm from either the C δ 2 atom or C ϵ 2 atom of Trp62. This cutoff is justified by the RDF between [EMIM] $^+$ CR and Trp62 C δ 2 or C ϵ 2, where the maxima occur at around this value (Figure S1). For the spatial distribution function figures, isovalues used for cation and anion in [EMIM][EtSO $_4$] are -0.01285 and -0.000586, respectively; isovalues used for cation and anion in [EMIM][Et $_2$ PO $_4$] are -0.019402 and 0.009118, respectively. All other analyses along with SDF were done with the inbuilt tools in Gromacs or VMD 33 . All structure images were rendered from VMD.

Results and Discussion

Calorimetric scans of lysozyme in IL-water solutions provide a great deal of information regarding the protein state and its transitions. A representative scan is shown in Figure S2. Upon heating, lysozyme shows a well-defined endothermic peak, consistent with thermally-induced protein unfolding. The location of this peak corresponds to the melting temperature T_m . Second, with appropriate baseline correction³⁴, the enthalpy of the transition ΔH is directly given by the area under the curve. Third, integration of the curve allows us to determine the transition width ΔT , an important parameter of the unfolding process³⁵.

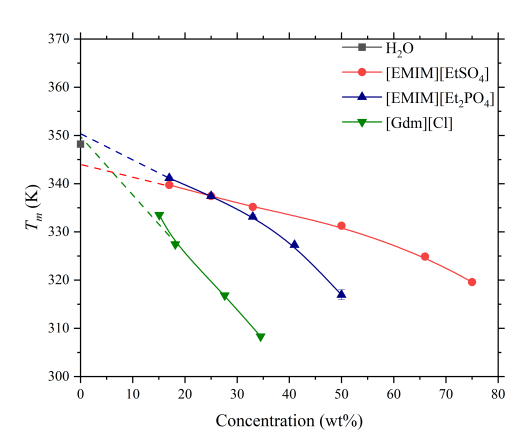


Fig. 2 Effect of IL concentration on lysozyme melting temperature T_m from calorimetry. For comparison, data for the effect of [Gdm][Cl] is also shown 36 .

Figure 2 shows how the lysozyme melting temperature T_m varies in the presence of both ILs. There is an initial linear regime, followed by a stronger decrease at higher IL content. This trend indicates a gradual effect of the ILs on lysozyme stability and is in contrast to strong denaturants, such as guanidinium chloride, which causes a rapid decrease in T_m and complete unfolding near room temperature $^{36-38}$. Comparing the effect of the two ILs, [EMIM][Et₂PO₄] lowers the lysozyme T_m more readily than [EMIM][EtSO₄], with the difference most noticeable above 30 wt% IL.

The thermal denaturation of lysozyme in other IL-water mixtures has been previously reported 3,9,39,40 . Specifically, calorimetric determinations of lysozyme T_m can either show a decrease or an increase with added IL. Such variation is not limited to lysozyme, as there are similar instances for RNaseA in IL-water mixtures 8,22 . It seems clear that there is no simple rule to explain such effects and instead we must turn attention to specific interactions between the IL ions and protein functional groups.

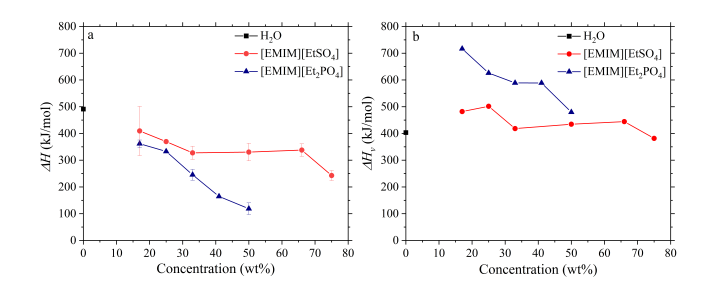


Fig. 3 Effect of IL concentration on the lysozyme (a) transition enthalpy ΔH and (b) effective transition enthalpy ΔH_{ν} from the van't Hoff equation.

The energy required for protein transitions can be directly measured by DSC. Figure 3 (a) shows how the lysozyme transition enthalpy ΔH varies in the presence of both ILs. With added [EMIM][EtSO₄], ΔH first gradually decreases and then reaches a plateau at intermediate concentrations. With added [EMIM][Et₂PO₄], ΔH decreases continuously with IL concentration. As with T_m , the difference between [EMIM][EtSO₄] and [EMIM][Et₂PO₄] is most noticeable above 30 wt% IL. The lower

values of ΔH indicates less heat (energy) is required to unfold lysozyme in [EMIM][Et₂PO₄], and the relative impact of this IL is more clearly seen in ΔH as compared to T_m .

The melting temperature T_m of a protein is often quoted as a measure of thermal stability, but from the relation $T_m = \Delta H/\Delta S$ it is seen that T_m reflects two quantities. In both [EMIM][EtSO₄] and [EMIM][Et₂PO₄] solutions, the decrease in lysozyme ΔH (Figure 3 (a)) is accompanied by a decrease in ΔS . Specifically for [EMIM][Et₂PO₄], the small ΔS at high IL concentrations is consistent with a smaller difference between the initial (folded) and final (unfolded) states, and suggests a "loose" initial structure.

The shape of the melting curve determines if the thermal transition reflects "all-or-none", partial, or aggregate unfolding 35,41,42. Intuitively it is understood that a small transition width ΔT is indicative of high cooperativity, whereas a large ΔT is indicative of low cooperativity, aggregation, or polymorphism. The van't Hoff equation $\Delta H_v/RT^2 = d \ln K/dT$, where *R* is the gas constant and K is the equilibrium constant, is used to calculate the transition enthalpy as $\Delta H_v = 4RT_m^2/\Delta T$. If the calculated ΔH_v equals the calorimetrically-measured ΔH , then the assumption of a two-state equilibrium is satisfied and the protein melts as a single cooperative unit. Comparing ΔH and ΔH_{ν} (Figure 3), we conclude that lysozyme in [EMIM][EtSO₄] melts nearly as an all-or-none process, whereas lysozyme in [EMIM][Et2PO4] melts in a complex fashion, possibly as aggregates 43. We note here that turbidity is observed for samples having very high IL content (> 66 wt% for [EMIM][EtSO₄] and > 40 wt% for [EMIM][Et₂PO₄]), however, these samples remain indefinitely stable suspensions (observed for several weeks).

Computationally, we observe a similar trend for lysozyme stability as with experiments. Figure 4 shows the fraction of native contacts, C-alpha root-mean-square-deviation ($C\alpha$ RMSD), and radius of gyration (Rg) time series for water, 25 wt% [EMIM][EtSO₄], and 25 wt% [EMIM][Et₂PO₄] at three temperatures. The starting configurations are folded structures taken right after NPT equilibration for each system. From fraction of native contacts and Cα RMSD at 300 K we see that lysozyme is folded at all times in all systems with RMSD staying at around 0.2 nm. Indeed, lysozyme is very stable thermally considering its rather small size 44-48. The reason why lysozyme in water has slightly lower fraction of native contacts can be attributed to the more flexible movements from the loops and turns as seen in the C-alpha root-mean-square-fluctuation (Cα RMSF) analysis (Figure S3). The suppression of RMSF of a protein in aqueous IL mixtures has also been found for xylanase in [EMIM][EtSO₄] ⁴⁹.

When the temperature increases to 370 K as shown in Figure 4 (b) and (e), destabilization of lysozyme is observed starting from around 250 ns for both ILs. This temperature is also the temperature where we start to see different states occur for water system and IL systems kinetically, i.e., lysozyme is partially unfolded in ILs, but still folded in water at around 250-400 ns. A C α RMSD cutoff of 0.4 nm is used to distinguish folded states and not folded states. This cutoff can be seen more clearly from the PMF plots at 370 K (Figure S4), where the folded basins and the intermediate basins $^{50.51}$ are separated by this cutoff. As the simulation time becomes longer, lysozyme in water also starts to partially un-

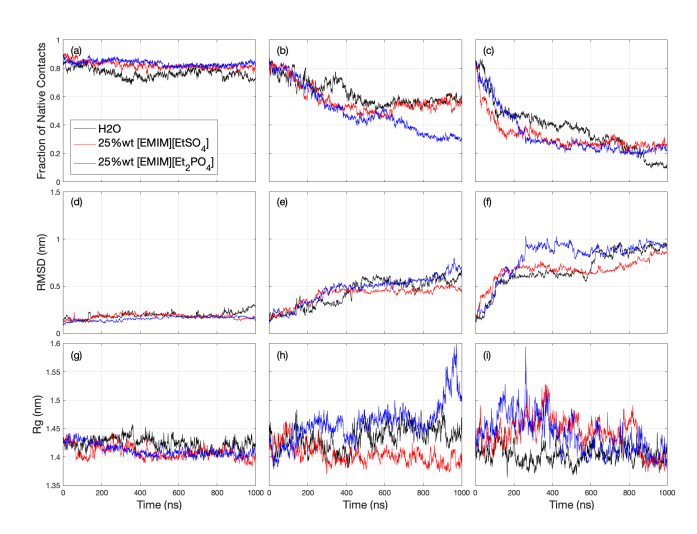


Fig. 4 Fraction of native contacts, RMSD, and R_g time series for water (black), 25 wt% [EMIM][EtSO₄] (red), and 25 wt% [EMIM][Et₂PO₄] (blue) systems. The first column is at 300 K, the second column is at 370 K, and the third column is at 400 K.

fold, while lysozyme in [EMIM][Et_2PO_4] further unfolds to have a fraction of native contacts of around 0.3. When temperature increases to 400 K, ILs still destabilize lysozyme faster than water does, as evident from the fraction of native contacts time series.

For R_g at 300 K, lysozyme in water has a slightly higher value compared to the other two systems, again possibly due to larger fluctuations in the loops and turns. At elevated temperatures, [EMIM][Et₂PO₄] has larger fluctuation in R_g compared to other two systems. This indicates that lysozyme in [EMIM][Et₂PO₄] samples more swollen conformations in not folded states.

As an experimental method to follow changes in lysozyme structure, we used intrinsic protein fluorescence. Lysozyme's fluorescence emission is predominantly due to tryptophan (Trp) residues ⁵². Out of the six Trp residues, only two of these (Trp62 and Trp108) are thought to contribute ¹⁶, the others (Trp28, Trp63, Trp111, and Trp123) are either buried within the hydrophobic core or quenched by nearby cysteine residues. Trp62 is especially important for lysozyme stability, since its mutation to glycine results in a lysozyme variant with disrupted long-range interactions ⁵³.

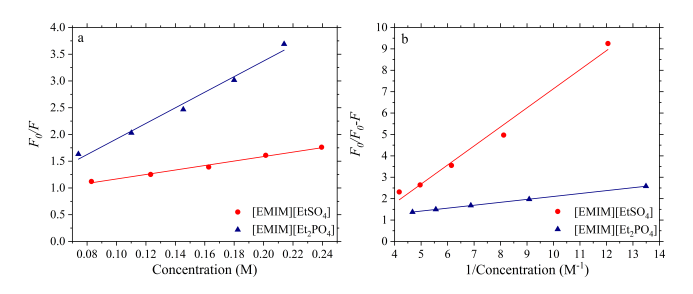


Fig. 5 (a) Stern-Volmer plot and (b) Lineweaver-Burk plot from fluorescence quenching of lysozyme with added IL.

The fluorescence data are presented in two ways: Stern-Volmer and Lineweaver-Burk plots (Figure 5 (a) and (b), respectively). In this manner we can discriminate between dynamic and static

quenching. Both the Stern-Volmer equation $F_0/F = 1 + K_{SV}[C]$ and the Lineweaver-Burk equation $1/(F_0-F) = 1/F_0 + 1/K_{LB}F_0[C]$ give their corresponding binding constants from the slopes of appropriate fits to the data. The fits to the experimental data are good, and Table 1 reveals that $K_{SV} > K_{LB}$, indicating a predominantly dynamic binding interaction between the ILs and lysozyme. This result is in contrast to a related study by Guo *et al.* ¹⁶, who used [BMIM][BF₄] and [BMIM][X] where [X] are halides. They found predominantly static binding with lysozyme, presumably due to the increased cation hydrophobicity in their study.

| System | K_{SV} , M^{-1} | K_{LB} , M |
|---------------------------------------|------------------------------|--------------|
| [EMIM][EtSO ₄] + lysozyme | 4.3 | 1.1 |
| $[EMIM][Et_2PO_4] + lysozyme$ | 14.5 | 7.3 |

Table 1 Binding constants obtained from Stern-Volmer and Lineweaver-Burk plots.

Table 1 shows that [EMIM][Et₂PO₄] has a larger binding constant than [EMIM][EtSO₄]. Although the effects of the IL cation and anion are complex, as we will discuss below, at least part of their destabilizing effect on lysozyme stability can be attributed to their difference in binding affinity with Trp. Indeed, the importance of Trp62 to lysozyme stability is thought to occur via a "sandwich-type" interaction between itself and two arginines (Arg73 and Arg113) 53,54 . A plausible mechanism of interaction between the ILs and Trp62 is through π - π and cation- π stacking between the [EMIM]⁺ cation's imidazolium ring and Trp62's indole ring. Such an interaction would compete with the native, and stabilizing, Arg-Trp-Arg sandwich.

Simulations allow us to directly observe the interactions of IL cations and anions at Trp62, and to confirm the competitive binding mechanism. Figure 6 shows the probability distribution of the absolute cosine angle between the normal of the [EMIM]+ ring and the normal of the Trp62 ring within a cutoff of 0.4 nm. The details of the calculation are described in the Experimental section. If the absolute cosine angle value equals to one, that means the rings are perfectly aligned with each other, and if the value equals to zero, that means the rings are perpendicular to each other. If we define the existence of the ring-ring alignment to have an absolute cosine angle value larger than 0.75, then for 25 wt% [EMIM][EtSO₄] is 89.80% aligned and for 25 wt% [EMIM][Et₂PO₄] is 83.91% aligned, which both indicate strong interaction between rings. The insets in Figure 6 show the spatial distribution function (SDF) of [EMIM]+ near lysozyme for the two ILs. From these figures the high density region of [EMIM]⁺ near Trp62 can be seen more readily.

The importance of Trp62 in lysozyme stabilization has been previously established both experimentally 53 but also in molecular dynamics simulations $^{55\,54}$. As mentioned earlier, our fluorescence data (Figure 5) lead us to presume that local π - π and cation- π stacking between [EMIM] ⁺ and Trp62 disturbs the native Arg73-Trp62-Arg113 interaction. Our simulation results directly confirm this IL-protein interaction (Figure 6). Furthermore, this mechanism explains why lysozyme is destabilized in both ILs studied here: both ILs share the same [EMIM] ⁺ cation. This in-

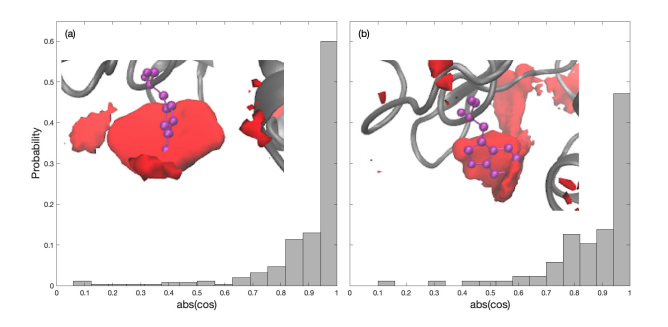


Fig. 6 The probability distribution of absolute cosine between the normal of [EMIM] $^+$ ring and the normal of Trp62 ring within a cutoff of 0.4 nm. The insets are SDF (200 ns-1 μ s) of [EMIM] $^+$ near the average structure of Trp62 (200 ns-1 μ s). (a) is in 25 wt% [EMIM][EtSO₄] and (b) is in 25 wt% [EMIM][Et₂PO₄]. Trp62 is shown in purple CPK representation.

terpretation is also consistent with the effect of [EMIM][Cl] on lysozyme 40 , which also reduces the T_m and hence destabilizes the protein (although to a lesser degree than either of the ILs here).

The significant role of the IL anions is clearly seen in Figure 2, and simulation provides additional evidence as to why anions are important in a global fashion. Because lysozyme is a highly charged basic protein with an isoelectric point pI $\approx 11^{56,57}$, it is expected that electrostatic interactions would be prominent in the protein's solubility and stability. Figure S5 shows the ratio between ILs and H_2O near protein and in bulk. The ratio between anions and H_2O near protein is greater than that in bulk in both IL systems, which indicates that more anions will partition to the protein surface. In contrast, the ratio between [EMIM] $^+$ and H_2O does not change that much near the protein and in bulk.

We next investigated how the specific anion contributes to the difference in lysozyme stability. Figure 7 shows the radial distribution function (RDF) between selected atoms of ILs and the whole protein. An illustration of the selected atoms is shown in Figure 1. A nearly identical trend is observed for [EMIM] + in both IL systems, indicating the similar distribution of [EMIM]⁺ near lysozyme and that the global distribution of [EMIM] + is not affected by the difference in anions. In addition, the cation peaks are less distinct compared to the anion peaks, indicating the distribution of [EMIM] + with respect to the protein surface is more delocalized. For the anions, [Et2PO4] - shows a strong orientational effect with phosphorous pointing towards the protein surface (Figure 7(b)), while for [EtSO₄] - the peaks are less distinct (Figure 7(a)), reflecting this anion's smaller dipole moment. For the same reason, the first coordination shell of [Et₂PO₄] - is closer to the lysozyme surface than $[EtSO_4]^-$.

The short-range interaction energies between ILs and the protein are further examined in Table 2. The cutoff of these two short-range interactions is set at 1 nm. Again, there is no clear difference in Coulomb and Lennard-Jones (LJ) interactions between [EMIM] $^+$ and protein in the two IL systems. However, the Coulomb short-range interaction is more than two times stronger between $[\mathrm{Et}_2\mathrm{PO}_4]^-$ and protein than between $[\mathrm{Et}\mathrm{SO}_4]^-$ and protein, which agrees with the observation in RDF that $[\mathrm{Et}_2\mathrm{PO}_4]^-$ has a closer first coordination shell. The two IL anions $[\mathrm{Et}\mathrm{SO}_4]^-$ and $[\mathrm{Et}_2\mathrm{PO}_4]^-$ differ in several ways, including that

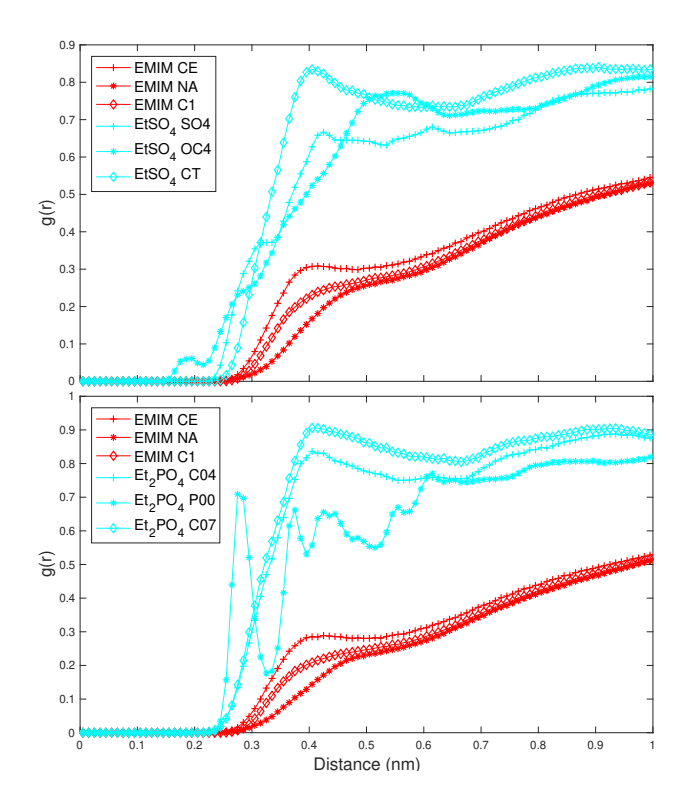


Fig. 7 RDF between selected atoms of ILs and the whole protein in (a) 25 wt% [EMIM][EtSO₄] and (b) 25 wt% [EMIM][Et $_2$ PO $_4$]. An illustration of the marked atoms is shown in Figure 1.

 $[{\rm Et_2PO_4}]^-$ has less charge delocalization and greater hydrophobicity than $[{\rm EtSO_4}]^-$, providing greater driving forces for interactions with both the protein surface charges and the hydrophobic interior. Since the interaction between the anion and the protein is stronger in $[{\rm EMIM}][{\rm Et_2PO_4}]$ than in $[{\rm EMIM}][{\rm EtSO_4}]$, this is another contribution causing the former system to be more destabilizing than the latter one.

Having identified important roles for both the IL cations and the IL anions, we turn our attention to their roles when together. Figure 8 shows the SDF of ILs near lysozyme, where lysozyme is shown in gray, red regions correspond to high density of [EMIM]+ and cyan regions correspond to high density of [EtSO₄] or [Et₂PO₄]. We observe that instead of being a homogeneous mixture like the bulk solution, the IL ions distribute in patches across different parts of the lysozyme surface. In both IL systems, positive residues attract anions and negative residues attract cations. In addition, some hydrophobic residues on the protein surface also attract both cations and anions, possibly due to the fact that both the cations and anions have at least one hydrophobic alkyl chain. This non-uniform distribution of ions near the protein surface suggests that there is no "universal" IL solvent for proteins, but rather, that each protein will need a uniquely tailored IL for optimum solubility and stability.

Conclusions

The interactions between lysozyme and two ILs, $[EMIM][EtSO_4]$ and $[EMIM][Et_2PO_4]$, are investigated with a combination of experiment and simulation. We find that lysozyme is destabilized

| Energy Type | Average (kJ/mol) | Standard Deviation (kJ/mol) | |
|---|------------------|-----------------------------|--|
| 25 wt% [EMIM][EtSO ₄] | | | |
| Coulomb (SR) Protein-EMIM | -40.96 | 35.87 | |
| LJ (SR) Protein-EMIM | -274.78 | 43.72 | |
| Coulomb (SR) Protein-EtSO ₄ | -1389.5 | 230.15 | |
| LJ (SR) Protein-EtSO ₄ | -575.76 | 74.33 | |
| 25 wt% [EMIM][Et ₂ PO ₄] | | | |
| Coulomb (SR) Protein-EMIM | -57.15 | 40.03 | |
| LJ (SR) Protein-EMIM | -225.21 | 42.04 | |
| Coulomb (SR) Protein-Et ₂ PO ₄ | -3082.48 | 383.67 | |
| LJ (SR) Protein-Et ₂ PO ₄ | -450.96 | 85.35 | |

Table 2 Short-range interaction between ILs and lysozyme.

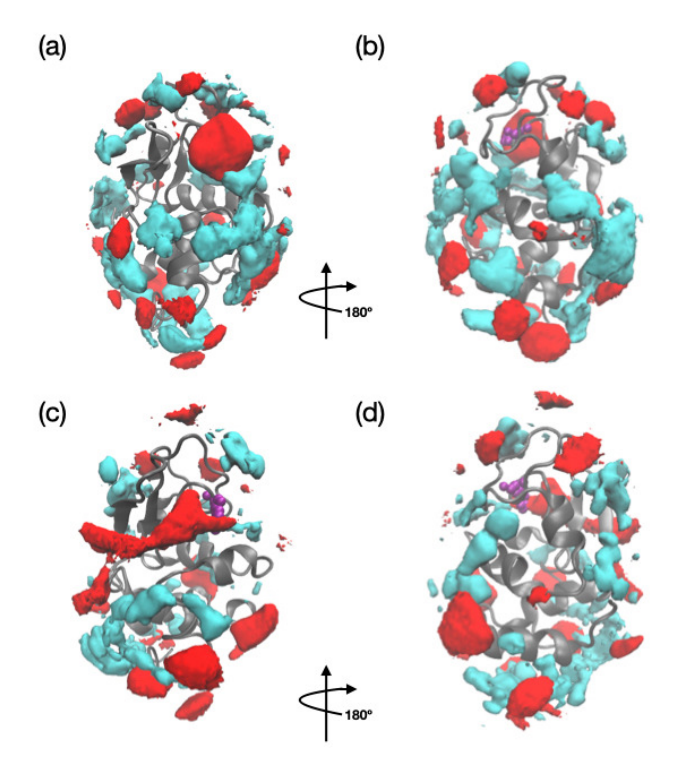


Fig. 8 SDF of ILs near lysozyme where red represents $[EMIM]^+$ and cyan represents anions: $[EtSO_4]^-$ in (a), (b) and $[Et_2PO_4]^-$ in (c), (d). Trp62 is shown in purple CPK representation. Panels (b) and (d) are after a rotation of approximate 180° of (a) and (c), respectively.

in the presence of ILs due to contributions from both the cations and anions, acting in local and global manners, respectively. The [EMIM] $^+$ cation exerts its effect locally by binding to tryptophan and presumably competing with a native Arg-Trp-Arg bridge that is critical to lysozyme stability, via favorable $\pi\text{-}\pi$ and cation- π interactions. The anions [EtSO4] $^-$ and [Et2PO4] $^-$, exert their effects globally through electrostatic effects, with the latter having the stronger short-range interaction. The differences due to the anions are likely due to the lower charge delocalization and greater hydrophobicity of [Et2PO4] $^-$. The protein surface het-

erogeneity is reflected in IL patterning, indicating no universal IL solvent for ILs, but rather, the need for each protein to have tailored ILs. Future investigations will benefit from combinated experiment and simulation, both to guide designer ILs but also to understand why some ILs outperform others.

Conflicts of interest

There are no conflicts to declare.

Acknowledgements

We acknowledge financial support from the National Science Foundation (CBET-1800442 for OS and HB and CBET-1760879 for PL and SM).

Notes and references

- 1 F. van Rantwijk and R. A. Sheldon, *Chemical Reviews*, 2007, **107**, 2757–2785.
- 2 J. R. Swartz, Current Opinion in Biotechnology, 2001, 12, 195–201.
- 3 H. Weingärtner, C. Cabrele and C. Herrmann, *Physical Chemistry Chemical Physics*, 2012, **14**, 415–26.
- 4 A. Schindl, M. L. Hagen, S. Muzammal, H. A. D. Gunasekera and A. K. Croft, *Frontiers in Chemistry*, 2019, **7**, 1–31.
- 5 J. Lloyd, P. Lydon, R. Ouhichi and M. Zaffran, *Vaccine*, 2015, 33, 902–907.
- 6 T. Takekiyo, K. Yamazaki, E. Yamaguchi, H. Abe and Y. Yoshimura, *Journal of Physical Chemistry B*, 2012, **116**, 11092–7.
- 7 E. C. Wijaya, F. Separovic, C. J. Drummond and T. L. Greaves, *Physical Chemistry Chemical Physics*, 2016, **18**, 25926–25936.
- 8 D. Constantinescu, H. Weingärtner and C. Herrmann, *Angewandte Chemie International Edition*, 2007, **46**, 8887–8889.
- 9 N. Byrne and C. A. Angell, *Journal of Molecular Biology*, 2008, **378**, 707–714.
- 10 K. Fujita, D. R. MacFarlane and M. Forsyth, *Chemical Communications*, 2005, 4804–6.
- 11 S. N. Baker, H. Zhao, S. Pandey, W. T. Heller, F. V. Bright and G. A. Baker, *Physical Chemistry Chemical Physics*, 2011, **13**, 3642–4.
- 12 I. Jha and P. Venkatesu, ACS Sustainable Chemistry & Engineering, 2015, 4, 413–421.
- 13 F. J. Deive, A. Rodríguez, A. B. Pereiro, J. M. M. Araújo, M. A. Longo, M. A. Z. Coelho, J. N. C. Lopes, J. M. S. S. Esperança, L. P. N. Rebelo and I. M. Marrucho, *Green Chem.*, 2011, 13, 390–396.
- 14 Q. Han, X. Wang and N. Byrne, *ChemCatChem*, 2016, **8**, 1551–1556.
- 15 U. K. Singh, M. Kumari, S. H. Khan, H. B. Bohidar and R. Patel, *ACS Sustainable Chemistry & Engineering*, 2018, **6**, 803–815.
- 16 Y. Guo, B. Zhang, C. Lu, X. Liu, Q. Li, H. Zhang and Z. Wang, Spectrochimica Acta Part A: Molecular and Biomolecular Spectroscopy, 2019, 214, 239–245.
- 17 M. Kumari, U. K. Singh, I. Beg, A. M. Alanazi, A. A. Khan and R. Patel, *Journal of Molecular Liquids*, 2018, **272**, 253–263.

- 18 J. P. Mann, A. McCluskey and R. Atkin, Green Chemistry, 2009, 11, 785.
- M. Senske, D. Constantinescu-Aruxandei, M. Havenith,
 C. Herrmann, H. Weingärtner and S. Ebbinghaus, *Physical Chemistry Chemical Physics*, 2016, 18, 29698–29708.
- 20 N. Byrne, L.-M. Wang, J.-P. Belieres and C. A. Angell, *Chemical Communications*, 2007, 2714–6.
- 21 K. D. Weaver, R. M. Vrikkis, M. P. Van Vorst, J. Trullinger, R. Vijayaraghavan, D. M. Foureau, I. H. McKillop, D. R. Mac-Farlane, J. K. Krueger and G. D. Elliott, *Physical Chemistry Chemical Physics*, 2012, 14, 790–801.
- 22 D. Constatinescu, C. Herrmann and H. Weingärtner, *Physical Chemistry Chemical Physics*, 2010, **12**, 1756–1763.
- 23 J. V. Rodrigues, V. Prosinecki, I. Marrucho, L. P. N. Rebelo and C. M. Gomes, *Physical Chemistry Chemical Physics*, 2011, 13, 13614–6.
- 24 T. Hunter, *Philosophical Transactions of the Royal Society B: Biological Sciences*, 2012, **367**, 2513–2516.
- 25 B. Hess, C. Kutzner, D. Van Der Spoel and E. Lindahl, *Journal of chemical theory and computation*, 2008, **4**, 435–447.
- 26 W. L. Jorgensen, D. S. Maxwell and J. Tirado-Rives, *Journal of the American Chemical Society*, 1996, **118**, 11225–11236.
- 27 J. N. Canongia Lopes, A. A. Pádua and K. Shimizu, *The Journal of Physical Chemistry B*, 2008, **112**, 5039–5046.
- 28 L. S. Dodda, I. Cabeza de Vaca, J. Tirado-Rives and W. L. Jorgensen, *Nucleic acids research*, 2017, **45**, W331–W336.
- 29 D. A. Beck, R. S. Armen and V. Daggett, *Biochemistry*, 2005, 44, 609–616.
- 30 T. Darden, D. York and L. Pedersen, *The Journal of chemical physics*, 1993, **98**, 10089–10092.
- 31 M. Parrinello and A. Rahman, *Journal of Applied physics*, 1981, **52**, 7182–7190.
- 32 T. Hofman, A. Goldon, A. Nevines and T. M. Letcher, *The Journal of Chemical Thermodynamics*, 2008, **40**, 580–591.
- 33 W. Humphrey, A. Dalke and K. Schulten, *Journal of Molecular Graphics*, 1996, **14**, 33–38.
- 34 W. M. Jackson and J. F. Brandts, *Biochemistry*, 1970, 9, 2294–2301.
- 35 A. V. Finkelstein and O. B. Ptitsyn, *Protein physics: a course of lectures*, Academic Press, 2016.
- 36 K. Ogasahara and K. Hamaguchi, *The Journal of Biochemistry*, 1967, **61**, 199–210.
- 37 K. C. Aune and C. Tanford, *Biochemistry*, 1969, **8**, 4579–4585.
- 38 Z. Xia, P. Das, E. I. Shakhnovich and R. Zhou, *Journal of the American Chemical Society*, 2012, **134**, 18266–18274.
- 39 C. A. Summers and R. A. Flowers, *Protein Science*, 2000, **9**, 2001–2008.
- 40 R. Buchfink, A. Tischer, G. Patil, R. Rudolph and C. Lange, *Journal of Biotechnology*, 2010, **150**, 64–72.
- 41 J. M. Sturtevant, Annual Review of Physical Chemistry, 1987, 38, 463–488.
- 42 P. L. Privalov and N. N. Khechinashvili, *Journal of Molecular Biology*, 1974, **86**, 665–84.
- 43 P. L. Privalov, Journal of Molecular Biology, 1996, 258, 707-

- 25.
- 44 C. Tanford, *Advances in Protein Chemistry*, Academic Press, 1968, vol. 23, pp. 121–282.
- 45 P. L. Privalov, Advances in Protein Chemistry, 1979, 33, 167–241.
- 46 O. B. Ptitsyn, *Advances in Protein Chemistry*, Academic Press, 1995, vol. 47, pp. 83–229.
- 47 *Lysozyme*, ed. E. F. Osserman, R. E. Canfield and S. Beychok, Academic Press, 1974.
- 48 *Lysozymes: Model Enzymes in Biochemistry and Biology*, ed. P. Jolles, Birkäuser, 1996.
- 49 V. W. Jaeger and J. Pfaendtner, *ACS chemical biology*, 2013, **8**, 1179–1186.
- 50 S. L. Kazmirski and V. Daggett, *Journal of molecular biology*, 1998, **284**, 793–806.
- 51 V. Daggett, Accounts of chemical research, 2002, 35, 422-429.

- 52 J. R. Lakowicz, *Principles of Fluorescence Spectroscopy*, Springer, 3rd edn, 2006.
- 53 J. Klein-Seetharaman, M. Oikawa, S. Grimshaw, E. Duchardt, T. Ueda, T. Imoto, L. Smith, C. Dobson and H. Schwalbe, *Science*, 2002, **295**, 1719–1722.
- 54 R. Zhou, M. Eleftheriou, A. K. Royyuru and B. J. Berne, *Proceedings of the National Academy of Sciences*, 2007, **104**, 5824–5829.
- 55 M. Eleftheriou, R. S. Germain, A. K. Royyuru and R. Zhou, Journal of the American Chemical Society, 2006, 128, 13388– 13395
- 56 Y. Desfourgères, T. Croguennec, V. Lechevalier, S. Bouhallab and F. F. Nau, *The Journal of Physical Chemistry B*, 2010, **114**, 4138–4144.
- 57 H. Yan, A. Nykanen, J. Ruokolainen, D. Farrar, J. E. Gough, A. Saiani and A. F. Miller, *Faraday Discussions*, 2008, **139**, 71.